International Journal of Science and Research (IJSR)
ISSN: 2319-7064
SJIF (2022): 7.942

Antibacterial and Antifungal Activity of Plant Mediated Iron Oxide Nanoparticles

Saraswathi Ramaiah Chinnasamy[1], Sujatha Dadhala[2], Anbarasan Veeran[3], Priyanka Ravichandran[4], Lakshmi Loganathan[5], Arivalagan Kuppusamy[6]

[1]Department of Chemistry, Government Arts College for Men (A), Chennai, Tamilnadu, India

[2]Department of Chemistry, Government Arts College for Men (A), Chennai, Tamilnadu, India

[3]Department of Chemistry, DMI College of Engineering, Chennai, Tamilnadu, India
Email:*kalicharan19982[at]gmail.com*

[4]Department of Chemistry, Dr. Ambedkar Govt. Arts College (A), Vyasarpadi, Chennai, Tamilnadu, India
Email:*priyaravi842[at]gmail.com*

[5]Department of Chemistry, Dr. Ambedkar Govt. Arts College (A), Vyasarpadi, Chennai, Tamilnadu, India
Email: *lakshmi251979[at]gmail.com*

[6]Department of Chemistry, Government Arts College for Men (A), Chennai, Tamilnadu, India
Email: *arivualagan16[at]gmail.com*

Abstract: ***In this study unexplored Albizia amara leaf extract was found to be capable in green synthesis of iron oxide nanoparticles and their characteristics were studied by using UV - Visible spectrometer, FT - IR, XRD, EDX, TEM and SAED pattern. Thus, biosynthesized iron oxide nanoparticles were naturally stabilised and in the size range of 100 - 200 nm with average particle size 160 nm. The phytochemicals present in the leaf extract has a main role as reducing agent that assists to the eco - friendly synthesis of iron oxide nanoparticles with enhanced antibacterial and antifungal activities. Well diffusion procedure was trailed to evaluate the antibacterial potential of green synthesized iron oxide nanoparticles against Bacillus subtilis, Escherichia coli, Klebsiella pneumoniae and Staphylococcus aureus. The antifungal property of synthesized iron oxide nanoparticles was evaluated against Candida albicans and Aspergillus niger. The naturally stabilized iron oxide nanoparticles with herbal property can be used in various biological application.***

Keywords: iron oxide nanoparticles, green synthesis, antibacterial activity antifungal activity and *Albizia amara* leaf extract

1. Introduction

The green synthesis approach is promising synthesis procedure in the research and development of materials science and technology due to the biosynthetic pathway of nanoparticle preparation, potentially eliminating the usage of hazardous chemicals and making the nanoparticles more biocompatible. Basic principles of green synthesis can be explained by the prevention or minimization of waste, reduction of pollutant derivatives, and the use of safer solvents as well as renewable feedstock [1]. The biomaterials extracted from several parts of the plant are mixed with metal precursor solutions under different reaction conditions for nanoparticle synthesis. The biomaterials play several roles such as reducing, capping and stabilizing agents in the synthesis of nanoparticles. Nanoparticles are produced within a few minutes or hours depending upon the type and concentration of biochemicals arising from plant sources. The plant extracts have been proven to possess high efficiency as stabilizing and reducing agents for the synthesis of nanoparticles but a detailed investigation of the role of reaction parameters in the synthesis is still needed to overcome existing problems in "green" synthesis [2].

Green methods involving plant parts extracts, algal, bacterial, and fungal forms are the most considered to produce various metal and metal oxide nanoparticles [3, 4]. These methods are environmentally safe, with short production times and low costs compared to other conventional methods. The synthesis of metal nanoparticles from plant extracts is considered an easy process relative to fungal and bacteria cultures since fungal and bacterial cultures requires sterilized conditions and skills to preserve. Furthermore, the plant extracts used to synthesize the nanoparticles show various size and shape distributions.

The phytochemicals include hydroxyl, carboxyl, and amino functional groups, which can serve both as effective metal – reducing agents and as capping agents to provide a robust coating on the metal nanoparticles in a single step [5, 6]. The synthesis of metal nanoparticles using inactivated plant tissue, plant extracts, exudates and other parts of living plants is a modern alternative for their production [7].

The various types of iron and iron oxide nanoparticles have been synthesized using extracts from plants and their parts, such as leaves, roots, flowers, bark, stems and seeds [8, 9], and iron oxide nanoparticles have several biomedical applications, such as magnetic beads in bacterial capturing, designing of sensor to detect various bio thread agents and being an instrumental in medical world. Therefore, we have reviewed the green chemistry type of iron and iron oxide nanoparticles synthesis process [10]. Biotechnology tools and techniques synthesize proteins, lipids, alkaloids, and flavonoids through biological routes, including microbes,

plants, and plant parts. [11, 12]. A graphical summary of biosynthesis nanoparticle synthesis is shown in Figure 1.

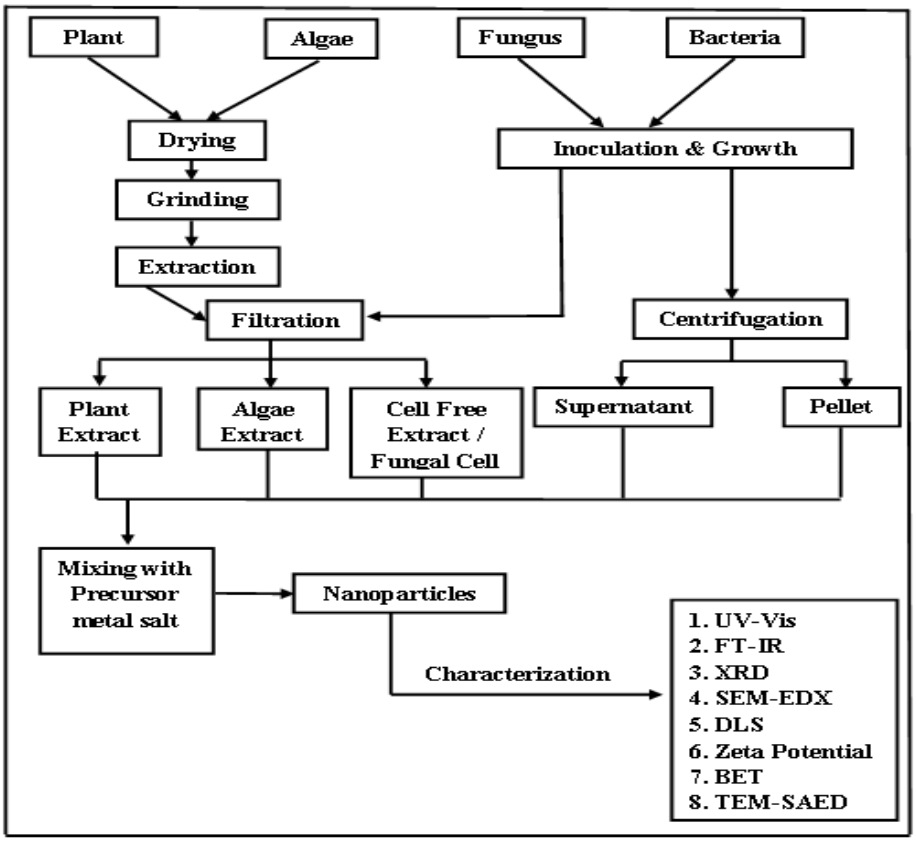

Figure 1: General Protocol for Biosynthesis of Nanoparticles

In this work, we carried out synthesis of iron oxide nanoparticles using ferric chloride as iron precursor and *albizia amara* leaf extract as reducing and capping agent. The synthesized iron oxide nanoparticles was investigated antimicrobial activity and antifungal activity.

2. Materials and methods

Albizia amara leaves were collected from local area in Chennai. All reactions are carried out with Borosil glassware's and double distilled water. The bacterial strains *Bacillus subtilis (*MTCC 441) and *Escherichia coli (*MTCC 443), *Klebsiella pneumoniae (*MTCC 109), *Staphylococcus aureus (*MTCC 96) and fungal strains *Aspergillus niger* (MTCC 404) and *Candida albicans* (MTCC 227) were obtained from MTCC, IMTECH, Chandigarh.

Preparation of *Albizia amara* leaf extract: Fresh leaves of *Albizia amara* were gathered, and subjected to multiple washes using tap water and subsequently with distilled water to eliminate any dust particles. The washed leaves were cut into a small pieces then dried for a period of 5 to 10 days in a covered area at room temperature. Once completely dried, the leaves were pulverized in an electronic blender to obtain a fine powder, which was then stored in an air tight container at room temperature for future use.10 grams of the obtained leaf powder was measured and placed in a 250 ml conical flask. To this 100 ml of double distilled water was added, and the mixture was heated at 80 to 90°C for 30 minutes. After the heating process, the aqueous leaf extract was filtered through Whatman filter paper No.1 and allowed to cool at room temperature. The filtrate was centrifuged at 1200 rpm for 15 minutes, after which it was filtered, the pale brown solution was adjusted to a pH=11 by adding 0.1M of NaOH solution, and then set aside for further processing. .

Synthesis of Iron Oxide Nanoparticles (FeONPs): In a 250 ml conical flask, 50 ml of *Albizia amara* leaves extract was taken and to this 50 ml of 0.1M $FeCl_3$ solution was gradually added at room temperature under static condition. The colour change was observed and the time taken for the reaction to occur was noted. As soon as iron oxide nanoparticles form, the colour of the solution changes from pale brownish to reddish brown. Further the solution was centrifuged and the obtained precipitate was dried in a hot air oven for 24 hours at 100ºC. The synthesized iron oxide nanoparticles kept in the muffle furnace at 350ºC for 4 hours.

Anti – microbial activity of iron oxide nanoparticles: The anti – microbial activities of iron oxide nanoparticles from the albizia amara leaf extract were evaluated the Agar Well Disc Diffusion method [13]. The agar well diffusion technique was used to assess the antibacterial efficacy of *Albizia amara* leaf extract mediated FeONPs against clinically relevant bacterial pathogens (*Escherichia coli, Klebsiella pneumoniae, Bacillus subtilis,* and *Staphylococcus aureus*). Using the agar well diffusion technique, FeONPs mediated by *Albizia Amara* leaf extract were evaluated for their antifungal efficacy against clinically relevant fungal pathogens (*Candida albicans* and *Aspergillus Niger*).

3. Results and Discussion

Characterization of Plant mediated synthesis of FeONPs

UV – vis studies

UV – vis spectrometry has revealed the characteristic formation of nanoparticles during colour change based on the absorption spectra. The formation of iron oxide nanoparticles was evidenced by the addition of aqueous ferric chloride solution to the leaf extract resulted in the appearance of an instantaneous dark black colour change from brown in the solution. This formation was due to a variety of plant biomolecules such as polyphenols, flavonoids, which played major role in the reduction of metal ions and sufficiently stabilized the iron oxide nanoparticles. As can be seen from Figure 2a, the absorption peaks for *Albizia amara* leaf extracts are around 370 to 390 nm, which corresponds to the existence of several natural compounds in the extracts [14]. These peaks are vanished after reacting with an iron salt, indicating that the extract compounds acted as reducing and capping agents to synthesize the iron oxide nanoparticles. Furthermore, and in accordance with the results of the present study, the surface plasmon band for iron oxide nanoparticles at wavelengths of 412 nm indicate the formation of iron oxide nanoparticles were reported by previous studies (Figure 2) [15].

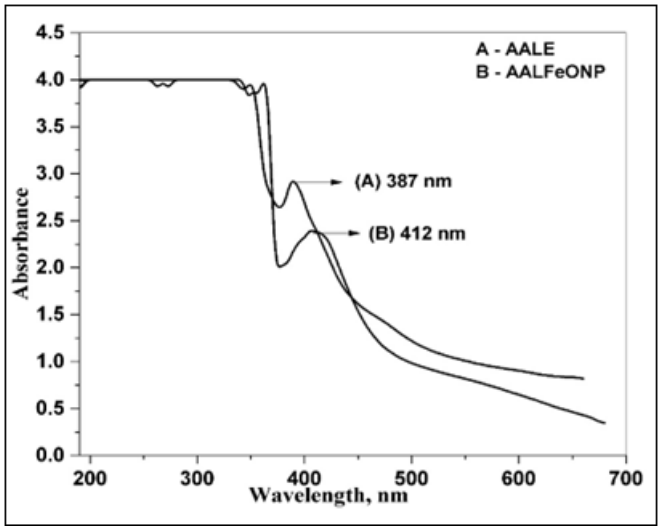

Figure 2: UV - Visible spectra of *Albizia amara* leaf extract and iron oxide nanoparticles

By utilizing the Planck's equation, the band energy gap of iron oxide nanoparticles has been calculated from UV - Vis spectrum (Equation 1),

$$E_{bg} = 1240 / \lambda \text{ (eV)} \quad (1)$$

λ - absorption maximum wavelength (nm)

From the above formula the E_{bg} value of iron oxide nanoparticles was found to be 3.00 eV [16].

FT - IR spectroscopy analysis

The FT - IR analysis were performed on the *Albizia amara* leaf extract and the synthesized iron oxide nanoparticles to identify a possible change in functional group bonds during the reduction process and presented in Figure 3.

Figure 2a, shows the IR spectrum for *Albizia amara* leaf extracts displayed prominent bands of absorbance at around 3391, 2069, 1639, 816 and 681 cm^{-1}. The same pattern was roughly observed for the synthesized iron oxide nanoparticles Figure 3b. The shifted absorption band observed at 561 cm^{-1}, for the *Albizia amara* leaf extract band at 681 cm^{-1} corresponds to Fe - O stretches of iron oxide confirming the formation of nanoparticles. The observed band were higher in intensity than the extract, confirming the reducing role of the extract in the formation of iron oxide nanoparticles. In Figure 3a, the peak near 1000 cm^{-1} corresponds to the stretching vibration of C - O - C, polyphenol compounds present in the plant extract. The absorption band at 1639 cm^{-1} related to the C=O bond stretching denotes polyphenol compounds and amino acids which stabilized and acted as a capping agent. Polyphenol compounds and phenyl groups play an essential role in reducing iron ions and then to iron oxide nanoparticles [17]. The band with higher intensity (Figure 2b) assigned to the - OH groups indicates water soluble polyphenol compounds that have capped the surface of the prepared iron oxide nanoparticles. The band at 2047 cm^{-1} may be due to C≡N stretching from unreacted impurities or due to CO_2 in the sample compartment. The band at 3393 $cm^{-1}$and 2800 cm^{-1} corresponds to the - OH bond stretching and denotes the aqueous phase, with an increase in the absorption band, indicating the ferrous sulphate reduction. The existing findings agreed well with the reported values [18].

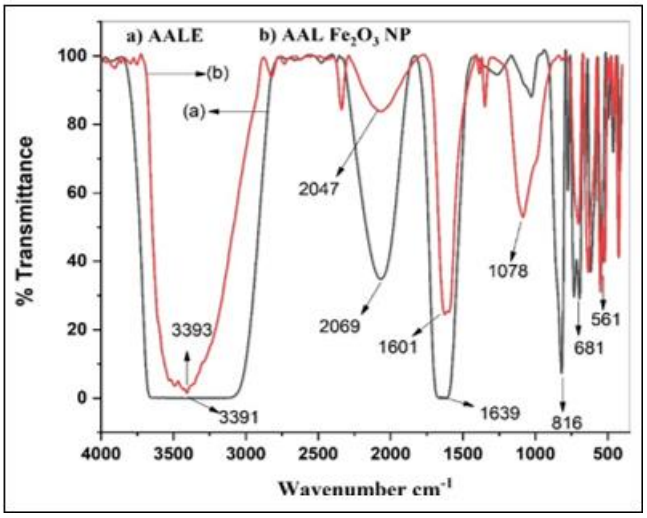

Figure 3: FT - IR spectra of a) *Albizia amara* leaf extract and b) iron oxide nanoparticles

X - ray diffraction (XRD) analysis

The XRD pattern of the *Albizia amara* leaf extract stabilized iron oxide nanoparticles shown in Figure 4. The XRD data as shown in Figure 4, shows six distinct peaks at 2 θ values of 35.12°, 36.63 °, 40.64 °, 49.97°, 57.08 ° and 65.49 ° with corresponding lattice plane values at (104), (110), (113), (024), (116) and (300) respectively. The intense and sharp peaks undoubtedly revealed that iron oxide nanoparticles formed by the reduction method using *Albizia amara* leaf extract were crystalline in nature. Furthermore, all these diffraction peaks are in good agreement with the database of standard ICPDS Card number 00 - 019 - 0629. The results are almost similar to

the results obtained for iron oxide nanoparticles by other researchers [19, 20].

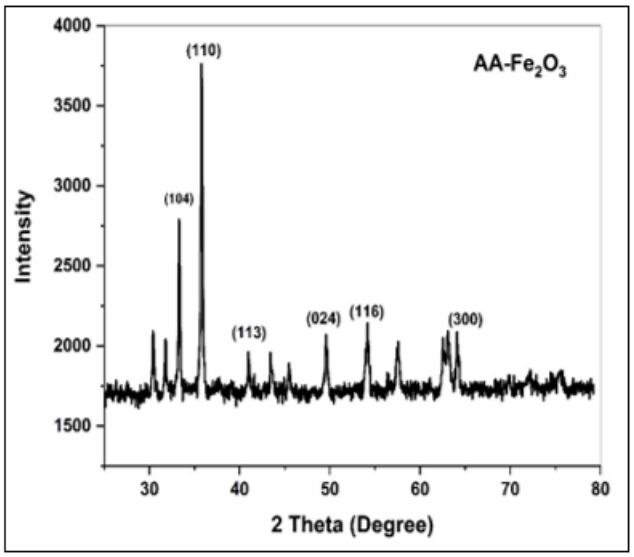

Figure 4: X - ray diffraction spectrum of iron oxide nanoparticles

Energy Dispersive X - Ray (EDX) microanalysis

The elemental composition of the green synthesized iron oxide nanoparticles was analysed by EDX analysis (Figure 5). The EDX analysis in Figure 5, clearly shows the presence of K - α lines at 6.4 KeV due to Fe atoms present in the nanoparticles and K - α lines at 0.6 KeV from O atoms and K - α lines at 2.7 from Cl peaks. Similar results were also obtained by previous studies [21]. Other tiny peaks, such as Keα lines at 0.24, 1.25 and 1.5 KeV are coming from Ca, Na and Al respectively. Presence of Cl as impurities is usually observed during iron oxide nanoparticles synthesized from ferric chloride as precursors. The Fe and Cl peaks might have originated from the FeCl3 precursors used in the fabrication of these iron oxide nanoparticles. The higher percentage of chlorine indicated the plant biomolecules present in the metal ions reduction and stabilization of the green synthesized iron oxide nanoparticles [22]. The percent of weight and atomic weight percentage are listed in Table 1.

Table 1: Constituent elements and their percentage values

Element	Line type	Weight %	Atomic %
O	K series	23.05	46.61
Cl	K series	10.28	9.38
Ca	K series	7.40	5.98
Fe	K series	52.38	30.34

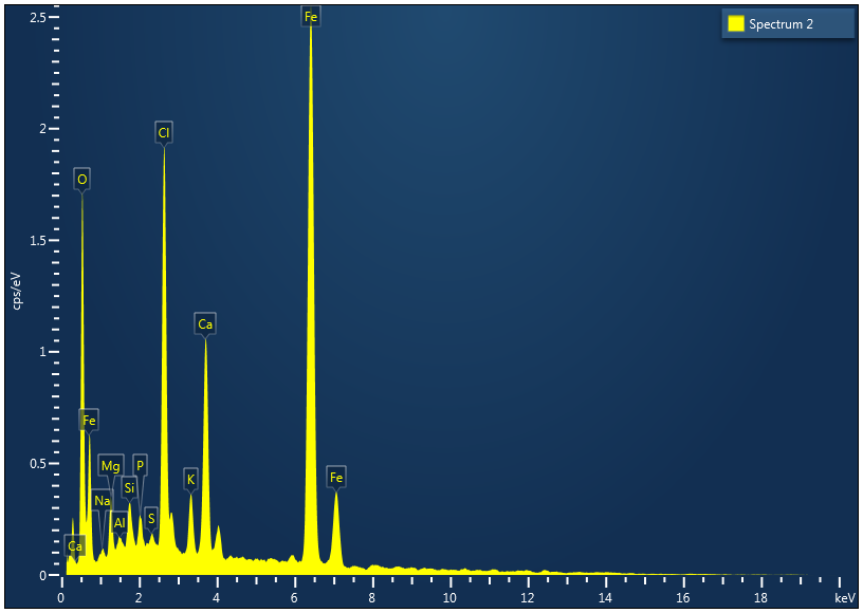

Figure 5: EDX spectrum of iron oxide nanoparticles

Transmission Electron Microscope (TEM) analysis

Figure 6, depicts a TEM images of iron oxide nanoparticles synthesized using *Albizia amara* leaf extract. The HR - TEM images of synthesized iron oxide nanoparticles and SAED pattern obtained from HR - TEM studies are depicted in Figure 6a - d, which give clear indications regarding size, shape and size distribution of nanoparticles. Figure 6a, shows the TEM images of iron oxide nanoparticles which reveals a polydispersity in shapes and sizes, with most nanoparticles of nearly spherical in shape, which agrees with XRD analysis [23].

HR - TEM shows (Figure 6b) the crystalline structure of single biogenic nanoparticles, with visible lattice fringes with springe spacing of 0.20 nm was calculated, corresponding to the plane family (111) of FCC iron. The particle size distribution and average size distribution is calculated from the Gaussian fitting of size distribution histogram of as shown in Figure 6c. The particle size distribution of biogenic synthesized FeO NPs ranges from 100 to 200 nm, where the average particle size is found to be 160 nm.

Moreover, the selected area electron diffraction (SAED) pattern (Figure 6d), which indicates their cubic crystallinity

nature and each of the diffraction rings has been indexed as (110), (113), (116) and (300). The SAED pattern of the single particle, the sharp diffraction spots (white dots in Figure 7d) clearly suggest the particle is of single crystal quality and the plane could be indexed to the FCC iron. The results are in agreement with XRD result as well. From the Figure 7d, the crystalline nature of green synthesized iron oxide nanoparticles is confirmed by the presence of bright spots. The concentric bright rings encompassing of small spots (Figure 7d) proved that the green synthesized iron oxide nanoparticles were highly crystalline and those were of cubic crystalline. These characteristic concentric rings with tiny spots symbolised the presence of planes corresponding to iron oxide nanoparticles [24].

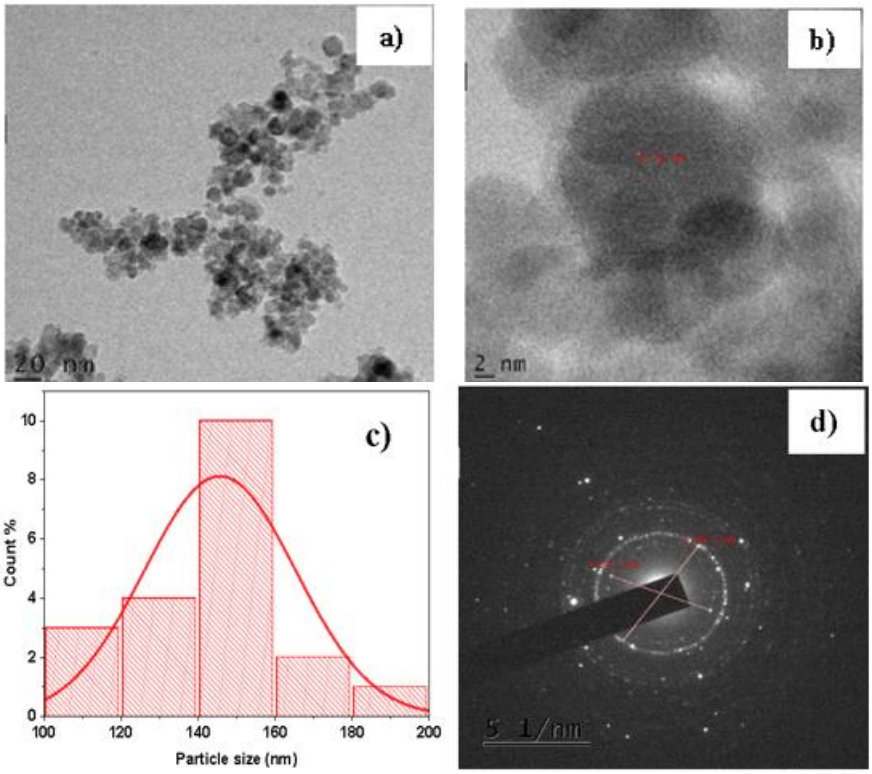

Figure 6: a) TEM image b) HRTEM image c) Particle size histogram and d) SAED pattern of green synthesized iron oxide nanoparticles

Anti - bacterial activity

Mueller - Hinton Agar well diffusion method

The antibacterial activity was determined by well diffusion methods [25]. Well diffusion procedure was trailed to evaluate the antibacterial potential of green synthesized iron oxide nanoparticles against *Bacillus subtilis, Escherichia coli, Klebsiella pneumoniae* and *Staphylococcus aureus*. The zone of inhibition (ZOI) around the wells were measured in mm using zone scale reader. The obtained results were exhibited in Figure 7. From the figure 7, the ZOI is increased as the dose of iron oxide nanoparticles is augmented. This represents the dose dependent antibacterial activity of iron oxide nanoparticles against clinically significant pathogens. Further, the results are analogous with standard antibacterial drug Azithromycin (30 µg/well). This displays that our synthesized nanomaterial is equal to standard antibacterial agent. Control (0 µg/mL) did not show any activity [25].

Green synthesized iron oxide nanoparticles are highly effective against both Gram - negative (*Escherichia coli* and *Klebsiella* pneumoniae) and Gram - positive (*Bacillus subtilis* and *Staphylococcus aureus*) bacterial microbes [25]. But highest antibacterial outcome is against Gram negative pathogens (*Escherichia coli* and *Klebsiella* pneumoniae) denoting the effectiveness of iron oxide nanoparticles ascribing cell structure of Gram - negative pathogens with superior level. Amongst the four microbes, *Klebsiella pneumoniae* was inhibited to higher level with the use of iron oxide nanoparticles. *Escherichia coli* was inhibited in a moderate level followed by *Staphylococcus aureus* and *Bacillus subtilis* and *Klebsiella pneumoniae* (Figure 8). Remarkably, our nanomaterial showed excellent antibacterial potential against all the pathogens similar to the standard Azithromycin.

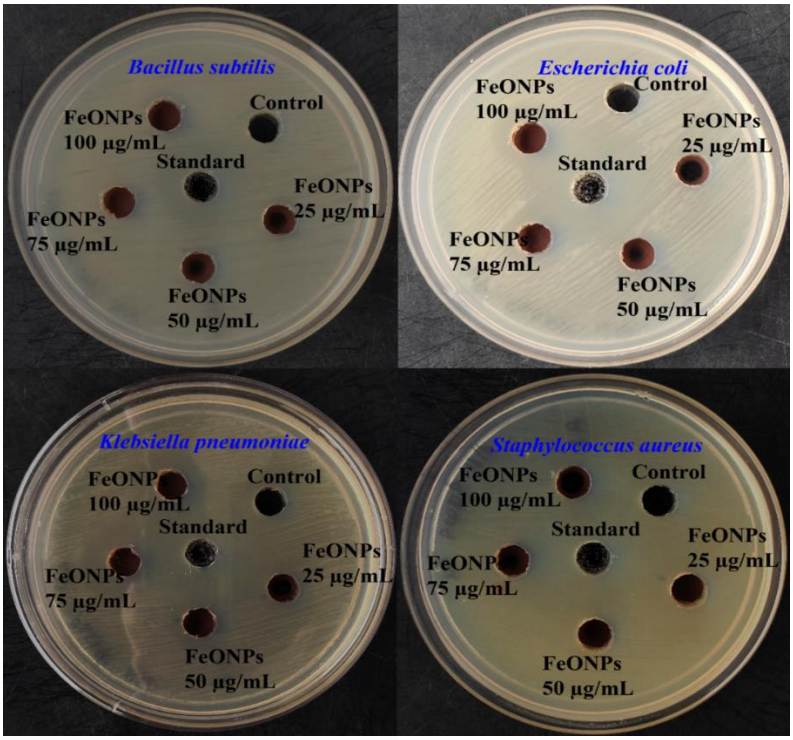

Figure 7: Well diffusion method antibacterial activity against *Bacillus subtilis, Escherichia coli, Klebsiella pneumoniae* and *Staphylococcus aureus* using green synthesized iron oxide nanoparticles (Control is 0 µg/mL) and Standard is Azithromycin 30 µg/well

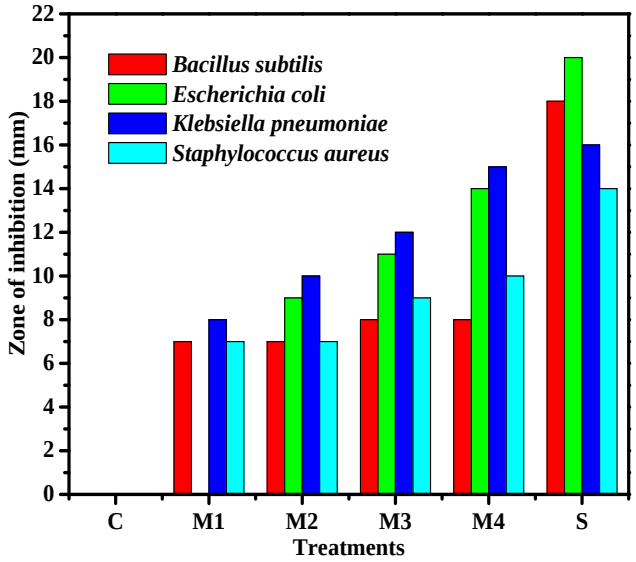

Figure 8: Antibacterial action of green synthesized iron oxide nanoparticles against *Bacillus subtilis, Escherichia coli, Klebsiella pneumoniae* and *Staphylococcus aureus* (C=0 µg/mL, M1=25 µg/mL, M2=50 µg/mL, M3=75 µg/mL, M4=100 µg/mL and S=Azithromycin 30 µg/well)

Anti - fungal activity

Potato Dextrose Agar well diffusion method

Well diffusion procedure was followed to assess the antifungal effectiveness of green synthesized iron oxide nanoparticles against *Candida albicans* and *Aspergillus niger*. The zone of inhibition (ZOI) around the wells were restrained in mm using zone scale reader. The attained data were displayed in Figure 9.

We could envisage that the ZOI is enhanced as the dosage of iron oxide nanoparticles is augmented. This verifies the dose dependent antifungal activity of iron oxide nanoparticles against medically noteworthy fungi. Additionally, the results are equivalent with standard antifungal agent Clotrimazole. This shows that our synthesized nanomaterial is similar with standard antifungal agent. Control (0 µg/mL) did not show any activity. Use of green synthesized iron oxide nanoparticles showed active antifungal activity against both *Candida albicans* and *Aspergillus niger*. But excellent antifungal effectiveness is against *Aspergillus niger* with improved level *(*Figure 10).

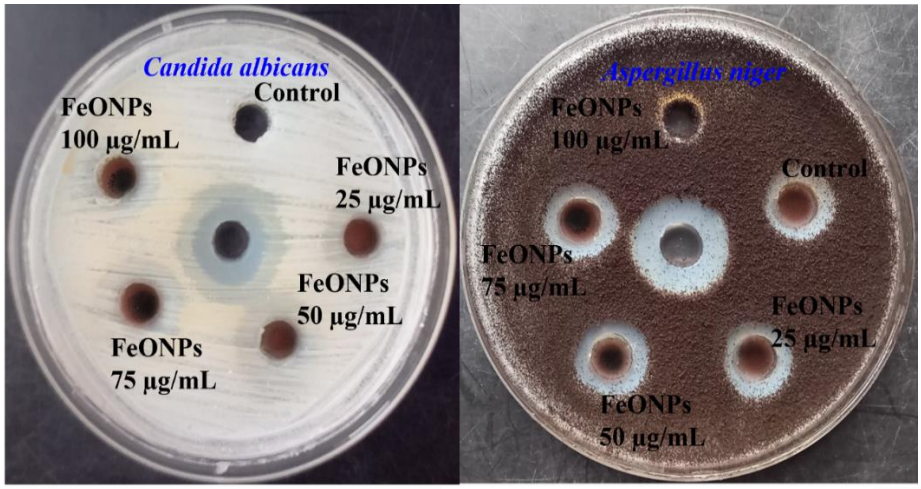

Figure 9.: Well diffusion method antifungal activity against *Candida albicans* and *Aspergillus niger* using green synthesized iron oxide nanoparticles (Control is 0 µg/mL) and Standard is Clotrimazole 30 µg/well

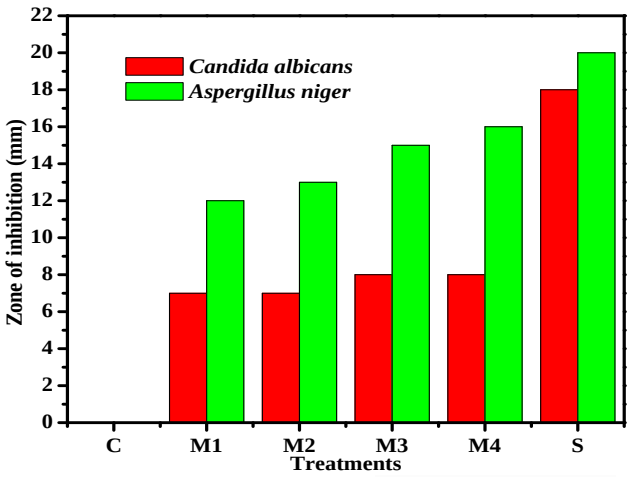

Figure 10: Antifungal action of green synthesized iron oxide nanoparticles against *Candida albicans* and *Aspergillus niger (*C=0 µg/mL, M1=25 µg/mL, M2=50 µg/mL, M3=75 µg/mL, M4=100 µg/mL and S=Clotrimazole 30 µg/well)

Reliable mechanism of antimicrobial activity using green synthesized FeONPs

Numerous constraints like shape, size, pH and capping agent plays enormous part in antibacterial ability. It is supposed that the biomolecules adhered to the exterior part of the nanomaterials plays major role in increase of bactericidal effectiveness [25]. Predominantly, iron oxide nanoparticles displays antimicrobial property due to the generation of reactive oxygen release (ROS) which leads to the damage to the membrane, impaired mitochondria, cell death, DNA damage, condensation in chromosome and inflammation (Figure 11). Betterment of antibacterial activity is determined based on the chemical moiety and release of metal ions from metal oxide [26].

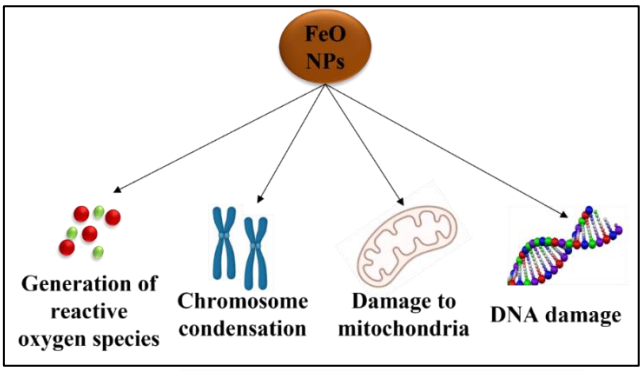

Figure 11: Schematic depiction of mechanism of antimicrobial activity using green synthesized iron oxide nanoparticles

References

[1] Singh J, Dutta T, Kim K, Rawat M, Samddar P and Kumar P, "Green synthesis of metals and their oxide nanoparticles: Applications for environmental remediation, " J. Nanobiotechnol., 2018, 16: 1 - 24.

[2] Herlekar M, Barve S and Kumar R, "Review article plant - mediated green synthesis of Iron nanoparticles, "J. Nanoparticle Res., 2014, 2014: 1 - 9.

[3] Virkutyte J and Vara R. S, "Chapter 2 Environmentally friendly preparation of metal nanoparticles, " in Sustainable preparation of metal nanoparticles: Methods and Applications, pp.7 - 33, The Royal Society of Chemistry, London, UK, 2013.

[4] Bhatttacharya D and Gupta R. K, "Nanotechnology and potential of microorganisms, " Critical Rev. in Biotech., 2005, 25: 199 - 204.

[5] Philip and Daizy, "Green synthesis of gold and silver nanoparticles using Hibiscus rosa sinensis, " Physica E: Low - dimensional Syst. Nanostr., 2010, 42: 1417 - 1424.

[6] Rahman A. S and Habibur, "Bottle Gourd (Lagenaria siceraria) – a vegetable for good health, " Nat. Prod. Radiance., 2003, 2: 249 - 250.

[7] Sivannarayana T, Saddam Hussain S. K and Phani Jithendra K, "Pharmacological and pharmaceutical applications of lagenaria siceraria (bottle guard), " Int. J. Inv. Pharm. Sci., 2013, 1: 288 - 292.

[8] Kumar B, Smita K, Galeas S, Sharma V, Guerrero V. H, Debut A and Cumbal L, "Characterization and application of biosynthesized iron oxide nanoparticles using citrus paradise peel: A sustainable approach, "Inorg. Chem. Comm., 2020, 119: Article ID 108116.
[9] Pallelaa P. N. V. K, Ummey S, Ruddaraju L. K, Gadi S, Cherukuri C. S, Barla S and Pammi S. V. N, "Antibacterial efficacy of green synthesized α - Fe_2O_3 nanoparticles using sida cordifolia plant extract, " Heliyon, 2019, 5: 1 - 7.
[10] Kumar A, Partap S and Sharma N, "Phytochemical, ethnobotanical and pharmacological profile of Lagenaria siceraria: A review, " J. Pharmacog. Phytochem., 2012, 1: 27 - 35.
[11] Singh P, Kim Y. J, Zhang D and Yang D. C, "Biological synthesis of Nanoparticles from plants and microorganisms, " Trends Biotechnol., 2016, 34: 588 - 599.
[12] Ovais M, Khalil A. T, Islam N. U, Ahmad K, Ayaz M, Saravanan M, Shinwari Z. K and Mukherjee S, "Role of plant phytochemicals and microbial enzymes in biosynthesis of metallic nanoparticles," Appl. Microbiol. Biotechnol., 2018, 102: 6799 - 6814.
[13] Khadayat K, Shepa D/D, Malla K. P, Shrestha S, Rana N, Marasini B. P, Khanal S, Rayamajhee B, Bhattarai B. R and Parajuli N, "Molecular identification and antimicrobial potential of streptomyces species from Nepalese soil, " Int. J. Microbiol., 2020, 2020: e8817467.
[14] Buarki F, AbuHassan H, Al Hannan F and Henari F. Z, "Green synthesis of iron oxide nanoparticles using hibiscus rosa sinensis flowers and their antibacterial activity, " J. of Nanotechnol., 20222022; 2022: 1 - 6.
[15] Mahdavi M, Namvar F, Ahmad M. B and Mohmad R, "Green Biosynthesis and Characterization of Magnetic Iron Oxide (Fe3O4) Nanoparticles Using Seaweed (Sargassum muticum) Aqueous Extract," Molecul. (2013; 18: 5954 - 5964.
[16] Das D, Nath B. C, Phukon P, Kalits A and Douli S. K, "Synthesis of ZnO Nanoparticles and Evaluation of Antioxidant and Cytotoxic Activity, " Colloids Surf. B Biointer.2013; 111: 556 - 560.
[17] Yardily A and Sunitha N, "Green synthesis of iron nanoparticles using hibiscus leaf extract, characterization, antimicrobial activity, " Inter. J. of Sci. Res. and Revie.2019; 8: 32 - 46.
[18] Demirezen D. A, Yilmaz S and Yilmaz D. D, "Green synthesis and characterization of iron nanoparticles using Aesculus hippocastanum seed extract, " Inter. J. of Adv. in Sci. Engg. and Tech.2018; 62: 24 - 29.
[19] Ahmmad B, Leonard K, Islam S, Kurawaki J, Muruganandham M, Ohkubo T and Kuroda Y, "Green synthesis of mesoporous hematite (α - Fe_2O_3) nanoparticles and their photocatalytic activity, " Adv. Power Technol.2013; 24: 160 - 167.
[20] Lassoued A, Lassoued M. S, Dkhil B, Ammar S and Gadri A, "Photocatalytic degradation of methylene blue dye by iron oxide (α - Fe_2O_3) nanoparticles under visible irradiation, Journal of material science, materials in electronics, " 2018: 29: 8142 - 8152.
[21] Kiwumulo H. F, Muwonge H, Ibingira C, Lubwama M, Kirabira J. B and Ssekitoleko R. T, "Green synthesis and characterization of iron - oxide nanoparticles using Moringa oleifera: a potential protocol for use in low and middle income countries, " BMC Res. Notes.2022; 15: 149 - 157.
[22] Qasim, S, Zafar A, Saif, M. S, Ali Z, Nazar M, Waqas M, Haq A. U, Tariq T, Hassan S. G, Iqbal F, Shu X. G and Hasan M, "Green synthesis of iron oxide nanorods using Withania coagulans extract improved photocatalytic degradation and antimicrobial activity, " J. Photochem. Photobiol. B: Biology.2020; 204: 111784.
[23] Newbury D. E, "Mistakes Encountered during Automatic Peak Identification in Low Beam Energy X - ray Microanalysis, " Scanning.2007; 29: 137 - 151.
[24] Swathi Pon S. S and George M, "In vitro anticancer and antitubercular activities of cellulose - magnetite nanocomposite synthesized using deep eutectic solvent as a dispersant, " J. Mater. Nano Sci.2021; 8: 1 - 10.
[25] Urnukhsaikhan E, Bold B. E, Gunbileg A, Sukhbaatar N and Mishig - Ochir T, "Antibacerial activity and characteristics of silver nanoparticles biosynthesized from Carduus crispus, " Scientific Reports, 2021, 11: 21047.
[26] Uchechukwu S. Ezealigo, Blessing N. Ezealigo, Samson O. Aisida, Fabian I. Ezema, JCIS Open, 2021, 4: 10002.